

Optimization of Machining Parameters on Electrochemical Micro Machining of Hastelloy C22 using Grey Taguchi Method

R. Manoj Samson^a, A.C. Arun Raj^a, T. Geethapriyan^a, S. Senkathir^a and S. Jenoris Muthiya^b

^aDept. of Mech. Engg., SRM University, Chennai, Tamil Nadu, India

^bDept. of Automobile Engg., Hindustan University, Chennai, Tamil Nadu, India

Corresponding Author, Email: jenoris.555@gmail.com

ABSTRACT:

Electro Chemical Machining (ECM) is a process that is used to machine extremely hard materials easily. It is a non-contact machining process. This ensures a higher tool life and no friction generated. The entire process is based on faradays laws of electrochemical process. With no heat affected zones (HAZ), this process holds a significant advantage over other high precision processes. This ensures that the material has neither thermal nor any other residual stresses. Nickel based alloys are known for their hardness and non-corrosive properties. This makes them unviable for machining using conventional methods as the overhead costs rise and makes them unproductive for use. ECM provides a better alternative comparatively. The alloy chosen for this analysis is Hastelloy C22. Its higher chromium content gives it better corrosion and pitting resistance. The objective of this analysis is to find the effects of various process parameters on MRR, surface finish, and dimensional deviation. The Taguchi technique has been used to investigate the effects of the ECMM process parameters and subsequently to predict sets of optimal parameters for maximum MRR and better surface finish. Grey analysis is done to find the optimal set of parameters for machining.

KEYWORDS:

Hastelloy C22; Machining; Material removal; Optimization

CITATION:

R.M. Samson, A.C.A. Raj, T. Geethapriyan, S. Senkathir and S.J. Muthiya. 2018. Optimization of Machining Parameters on Electrochemical Micro Machining of Hastelloy C22 using Grey Taguchi Method, *Int. J. Vehicle Structures & Systems*, 10(2), 108-114. doi:10.4273/ijvss.10.2.07.

1. Introduction

Electro Chemical Machining (ECM) is the generic term for a variety of electrochemical processes and it is one of the recent technologies [2-8]. In this processes electrolysis method is used to remove the metal from the work piece. It is best suited for metals and alloys which are difficult to be machined by mechanical machining processes. ECM is a contactless machining procedure in which the process is not subjected to tool wear, mechanical stresses, and micro-fissure. This process is used in aerospace industries, automotive, medical equipment, micro system and power supply industries [20]. Electro-chemical micromachining is considered to be a future micromachining technique since in many areas of application it offers several advantages that include higher machining rate, better precision and control, and a wider range of materials that can be machined. The finest approach to anodic dissolution processes is needed for electrochemical micromachining (ECMM) process to become widely using manufacturing process in the electronic and micro precision manufacturing [9-10].

The process of ECMM is presented in which side-insulated electrode, micro gap control between the cathode and anode. An experimental set-up for ECMM is constructed, which has machining technique gap control roles and also the pulsed power supply, the

control computer is involved. Microelectrodes are manufactured through micro electro-discharge machining (EDM) and side-insulated in chemical vapour deposition (CVD). A micro gap control strategy is proposed based on the essential experimental behaviour of electrochemical machining current with the gap change. Machining investigations taking place on micro whole drilling, scanning machining layer-by-layer, and micro electrochemical deposition are carried out. Preliminary experimental results show the feasibility of ECMM and its potential ability for better machining accuracy and smaller machining size. The output of theoretic and investigations of the relationship between the typical shapes, sizes and anode work piece surface by the micro-features of tool electrode are shown [17-19].

The results of an investigation of pulse micro-ECM using non-profiled electrodes are also conferred [11]. For successful utilization of ECMM process, it is necessary to analyze the following process criteria [12-16]:

- Material removal rate (MRR)
- Surface finish of the work piece
- Radial overcut of machined hole

In this work, the effect in MRR is analyzed, radial overcut and surface roughness (SR) is varied by the input parameters. Taguchi-grey analysis [1] is used to determine the optimum input process parameter to achieve a better surface finish with minimum radial overcut and good MRR.

2. Experimental setup and methodology

2.1. Experimental setup of ECMM

The setup comprises of various parts that can control one or more parameters of machining. Hence it is of vital importance to identify various components involved during machining of the work-piece. Fig. 1 shows the experimental setup of ECMM. The equipment consists of a tool holder. Since the tool is of various diameters, it plays an important role in handling the tool. It is connected to the servo motor which controls the drive of the tool. The tool holder can hold various types of the tool of various shapes and sizes. The entire work piece is placed in the electrolyte bath. It contains the flowing electrolyte and the work piece is attached to the setup inside the bath. It is submerged in the electrolyte. The dimensions of the bath are given as 200×100×80mm. It consists of the flow control valve and the flow control tube. It helps in maintaining the pressure and the flow of the electrolyte. A servomotor is a rotary actuator or linear actuator that allows for precise control of angular or linear position, velocity, and acceleration. It consists of a suitable motor coupled to a sensor for position feedback. It is a closed-loop servomechanism that uses position feedback to control its motion and final position. The input to its control is some signal, either analogue or digital, representing the position commanded for the output shaft. The pump is of the magnetic type. The primary objective of the pump is to drain the electrolyte contaminated with particulates, filter it and then re-pump it back into the system. The flow control system can later control the parameters. The filter comprises of a 5-micron cartridge that can be replaced from time to time. It is an important and most expensive part of the setup. It enables us the control of duty cycle and the frequency of the current supplied.



Fig. 1: Micro ECMM setup and pulse rectifier

2.2. Selection of materials

Hastelloy C22 is a nickel based super alloy. Its high chromium content at about 22% provides excellent corrosion resistance compared to other grades. The chemical composition of Hastelloy C22 is given in Table 1. The samples for machining are shown in Fig. 1.

Table 1: Composition of Hastelloy C22

Const.	% Comp.	Const.	% Comp.	Const.	% Comp.
C	0.006	Ni	57.018	V	0.021
Cr	22.187	P	0.013	Al	0.212
Co	0.097	Si	0.061	Ti	0.012
Fe	4.502	S	0.007	Cu	0.008
Mn	0.061	W	2.721	No	0.009
Mo	12.952				

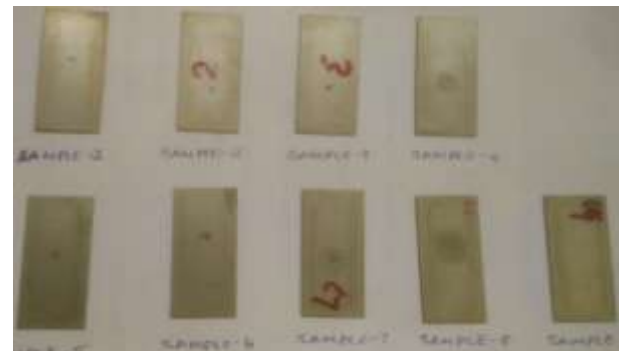


Fig. 2: Hastelloy C22 specimen

2.3. Methodology

Trial experiments of machining process are conducted to determine the range of each input parameters like applied voltage (V), current (A), electrolyte concentration (g/l), and duty cycle (%) that can be present before the actual experiment (see Table 2). After determining the range, the actual experiments (L9) are conducted by suitably varying the input parameters. Each experiment takes a different amount of time depending upon the parameters set for it and the capability of the machine. To better analyze the output parameter SR, a blind hole was drilled to get better access to the surface of the bottom of the hole. After the completion of each experiment, the work piece is carefully removed from the machining chamber and cleaned thoroughly to check for the micro blind hole which has been made by the machine. Since the blind hole was machined at the micro level, the size of the hole is small and it can be clearly seen through metallurgical microscope and diameter of each work piece sample can be measured from the metallurgical microscope. These measured diameter values of each work piece sample can be calculated as radial overcut, which will be useful in response measurement apart from MRR and SR as presented in Table 3.

Table 2: Input parameters and its levels

Factors	Level 1	Level 2	Level 3
Applied voltage (V)	8	10	12
Current (A)	2	3	4
Electrolyte concentration (g/l)	20	25	30
Duty cycle (%)	40	50	60

3. Result and discussion

Taguchi method can be adopted for optimizing the process variables. Analysis of variance is used to determine the percentage contribution of each optimization factor. The additive assumption implies that the individual or main effects of the independent variables on performance parameter are divisible. The design of experiments with optimization of control parameters to obtain best results is achieved in the Taguchi method.

3.1. Taguchi optimization

Taguchi optimization method is a single response optimization technique. It is a statistical method developed by Genichi Taguchi to improve the quality of engineered products. The exact values required are under-specified by the performance requirements of the system. This allows the parameters to be chosen so as to minimize the effects on performance arising from variation in manufacturing. Thus the arrangement of design of experiments with optimization of control parameters to obtain best results is achieved in the Taguchi Method as presented in Table 3. MRR and SR were found based on the given input parameters. The SR and radial overcut is better for the 1st work piece and the MRR is better for the 9th piece as observed. Orthogonal Arrays (OA) provide a set of well balanced (minimum) experiments and Signal-to-Noise ratios (S/N) serve as objective functions for optimization, help in data analysis and prediction of optimum results. For multi-response optimization, grey relation analysis coupled with Taguchi method is employed [1]. In this approach, the multi-response can be converted into a single normalized response.

3.2. Grey relation analysis

Conventional Taguchi method deals with single response optimization only. It may give a different set of optimal combination for multi-response. Therefore, it is needed to introduce multi-response optimization technique in the process. In this approach, the multi-response can be converted into a single normalized response. Grey relation analysis (GRA) is followed by five basic steps:

- Transform the response into the S/N ratio using the appropriate equation depending on the quality characteristics.
- Normalize the S/N ratio to distribute the data evenly and scale it into an acceptable range for further analysis. As per GRA, the normalized S/N ratio for larger the better case (MRR) is given by,

$$Z_{nj} = (Y_{nj} - \min Y_{nj}) / (\max Y_{nj} - \min Y_{nj})$$
 Similarly, the normalized S/N ratio for smaller the better case (SR and radial overcut) is given by,

$$Z_{nj} = (\max Y_{nj} - Y_{nj}) / (\max Y_{nj} - \min Y_{nj})$$
 Where, Z_{nj} is the normalized value of n^{th} trail for j^{th} dependent response.
- Compute the grey-coefficient for the normalized S/N ratio values using,

$$GC_{nj} = (\psi_{\min} + \delta \psi_{\max}) / (\psi_{nj} + \delta \psi_{\max})$$
 Where, GC_{nj} is the grey co-efficient for n^{th} trail for j^{th} dependent response. δ is the quality loss, ψ is the distinctive co-efficient which has value from 0 to 1.
- Compute the grey relational grade using,

$$G_n = (1/Q) \sum GC_{nj}$$
 Where, Q is number of response = 4, GC_{nj} is the grey co-efficient for n^{th} trail for j^{th} dependent response.
- Utilize response graph method to select the optimal levels of the input factors based on maximum average value (see Table 4 for ECMM process).

Table 3: Orthogonal array with MRR, SR and radial overcut

Sample No.	Voltage (V)	Current (A)	Electrolyte concentration (g/l)	Duty cycle (%)	MRR×10 ⁻² (mm ³ /min)	SR (μm)	Radial overcut (μm)
1	8	2	20	40	1.825	0.500	59.768
2	8	3	25	50	0.936	0.668	165.856
3	8	4	30	60	0.307	0.711	200.229
4	10	2	25	60	0.408	0.679	329.416
5	10	3	30	40	1.755	0.728	652.619
6	10	4	20	50	0.977	0.635	441.204
7	12	2	30	50	0.760	3.120	286.367
8	12	3	20	60	0.276	0.873	118.232
9	12	4	25	40	1.969	2.770	634.649

Table 4: Grey relational co-efficient with their rank

MRR (mm ³ /min)		SR (μm)		Radial overcut (μm)		Grey relational coefficient			Grey relational grade	Rank
S/N ratio	Normalized S/N ratio	S/N ratio	Normalized S/N ratio	S/N ratio	Normalized S/N ratio	MRR×10 ⁻² (mm ³ /min)	SR (μm)	Radial overcut (μm)		
5.23	0.961	6.02	0	-35.53	0	0.928	0.333	0.333	0.532	5
-0.57	0.621	3.50	0.158	-44.39	0.426	0.569	0.373	0.466	0.469	6
-10.26	0.054	2.96	0.192	-46.03	0.505	0.346	0.382	0.503	0.410	8
-7.79	0.198	3.36	0.167	-50.36	0.714	0.384	0.375	0.636	0.465	7
4.89	0.941	2.76	0.205	-56.29	1	0.895	0.386	1.000	0.760	2
-0.20	0.643	3.94	0.130	-52.90	0.836	0.584	0.365	0.753	0.567	4
-2.38	0.515	-9.88	1	-49.14	0.655	0.508	1.000	0.592	0.700	3
-11.18	0	1.18	0.304	-41.45	0.285	0.333	0.418	0.412	0.388	9
5.88	1	-8.85	0.935	-56.05	0.988	1.000	0.885	0.977	0.954	1

3.3. Influence of process parameters on MRR

Duty cycle has the most effect on overall MRR as shown in Fig. 3. Among the set levels, voltage affects the MRR least. Current forms a similar trend when compared to the voltage with very minimal changes in the output. The MRR spikes a bit the EC at 25 g/l. This shows that at higher concentrations the MRR decreases gradually. At higher duty cycle the MRR decreases drastically. Hence it is recommended that the duty cycle percentage is maintained at lower levels to have higher productivity while the rest of the parameters can be maintained at intermediate values.

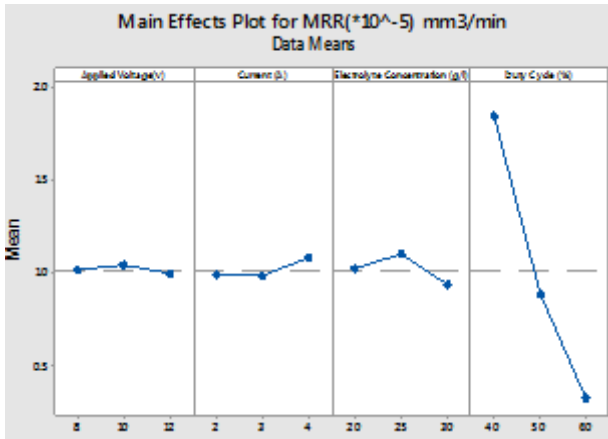
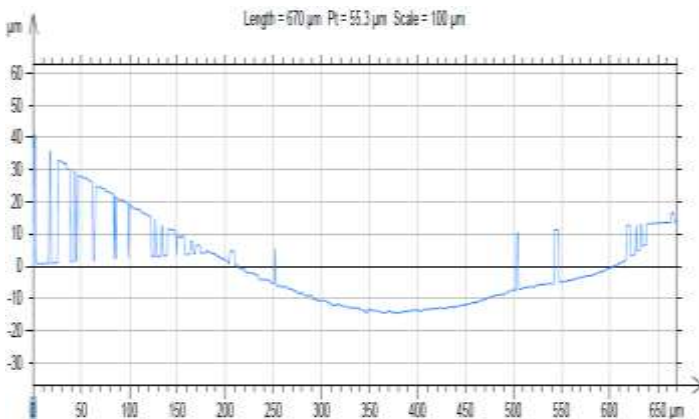


Fig. 3: Main effects plot for MRR

3.4. Influence of process parameters on SR

All parameters have a significant contribution to the given output value (SR) as shown in Fig. 4. Voltage and electrolyte concentration have a similar effect on surface roughness. At higher values of input, the quality of surface reduces significantly. The current plays an ambiguous role in the desired parameter with the value fluctuating but has a better surface quality at an intermediate value. Higher duty cycle values impart a better surface finish to the material. Voltage happens to be the major parameter affecting surface roughness overall. Maintaining a lower EC, voltage is paramount to obtain a better finish with the current at intermediate values and the duty cycle at the highest level. Fig. 5 represents the 2D & 3D graphical representation of surface roughness of the work piece, which provides the less accuracy result when the parameter of following



values are fixed: applied voltage is 8V, current is 2A, electrolyte concentration is 20g/lit and duty cycle is 40%. The given duty cycle value is low as opposed to the high values required. The current at its lowest point also plays a factor in reducing the overall quality of the surface. Duty cycle should be the major factor due to which poor surface finish is obtained in this material.

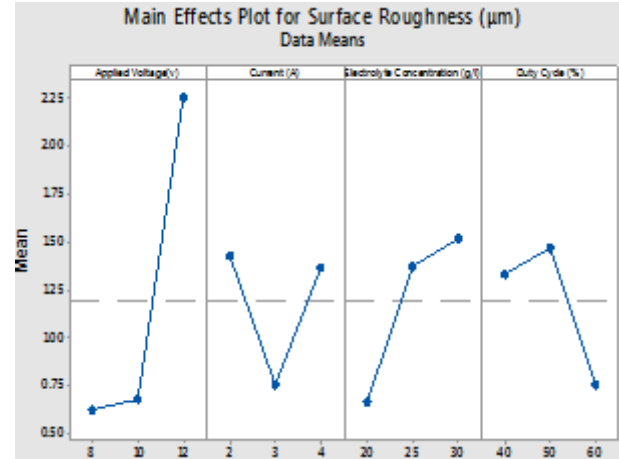


Fig. 4: Main effects plot for surface roughness

Fig. 6 represents the 2D & 3D graphical representation of surface roughness of the work piece (sample number) 8, which provide the optimal result when the parameter of following values are fixed: applied voltage is 12V, current is 3A, electrolyte concentration is 20g/lit and duty cycle is 60%. The minimal electrolytic concentration, intermediate current values provide for an optimal finish obtained in this sample. The duty cycle is also at its highest providing further finish for this piece. Hence duty cycle again plays a major factor coupled with minor contributions from current and electrolyte concentration. Fig. 7 represents the 2D & 3D graphical representation of surface roughness of the work piece (sample number) 9, which provide the better result when the parameters of following values are fixed: applied voltage is 12V, current is 4A, electrolyte concentration is 25g/lit and duty cycle is 40%. This gives a contradiction to all derived conclusions. But the highest duty cycle provides of the lowest MRR which may give a better surface finish to the product.

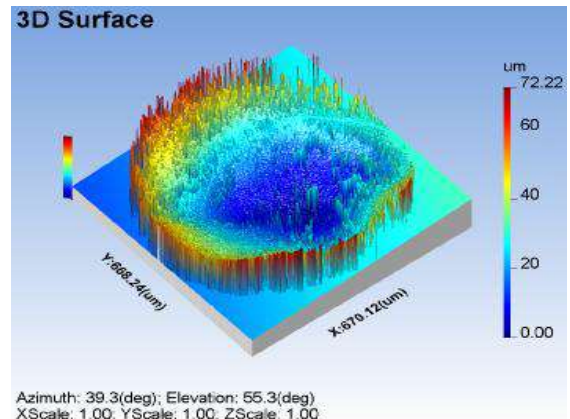


Fig. 5: 2D & 3D graph of surface roughness for less accuracy

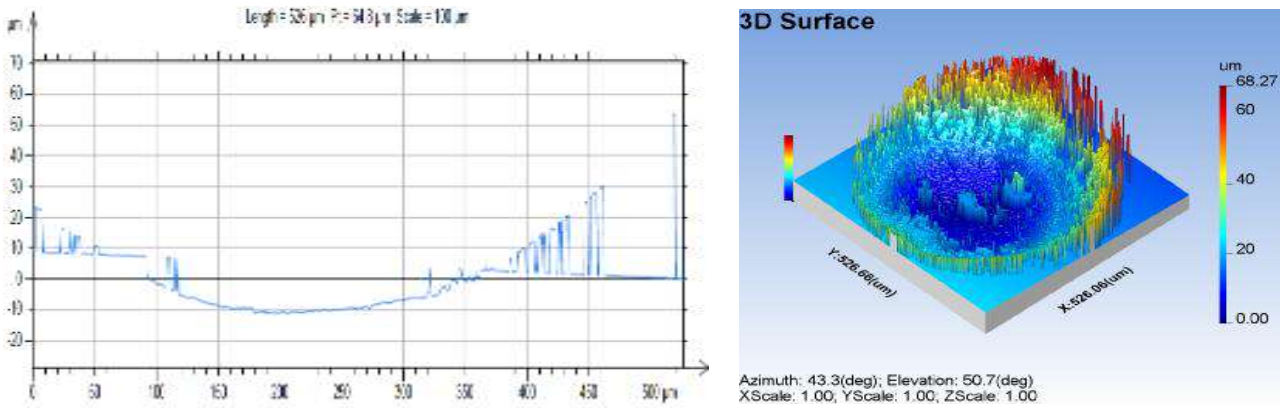


Fig. 6: 2D & 3D graphical representation of surface roughness for optimal

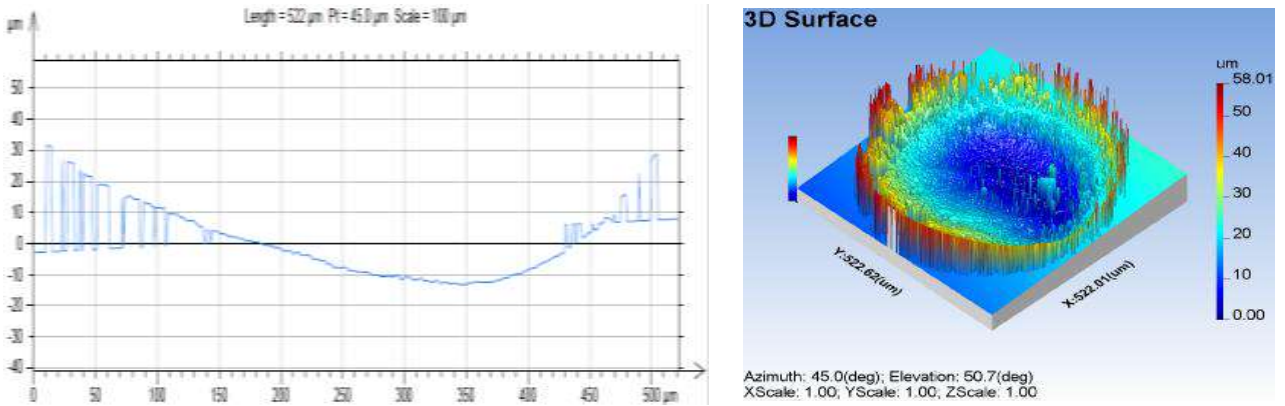


Fig. 7: 2D & 3D graphical representation of surface roughness for better

3.5. Influence of process parameter on radial overcut

All the parameters play a major factor in affecting the overcut. The value of the overcut fluctuates with the increasing levels of voltage. Both the current and EC increase the overcut as their value increases as shown in Fig. 8. The overcut decreases with increasing percentages of the duty cycle. Both voltage and duty cycle play a major role overall, in affecting the overcut. To get the least values of overcut, it is recommended to have lower values of voltage, EC, and current. The duty cycle can lie in the intermediate zone to obtain an acceptable level of overcutting. Fig. 9 represents the microscope image of the diameter of the work piece (sample number) 1, which provides the less accuracy result when the parameters of following values are fixed: applied voltage is 8V, current is 2A, electrolyte concentration is 20g/lit and duty cycle is 40%. All parameters are maintained at their lowest levels like required except duty cycle. A higher duty cycle can contribute towards a lower overcut but the values set for this work piece is at its lowest. Hence it could have played a major role in providing higher overcut values. Fig. 10 represents the microscope image of the diameter of the work piece (sample number) 9, which provide the better result when the parameters of following values are fixed: applied voltage is 12V, current is 4A, electrolyte concentration 25 is g/lit and duty cycle is 40%. The given duty cycle has a lower on time ratio providing for a lesser over the cut. Duty cycle combined with

intermediate electrolyte concentration provides a better current flow, giving a better finish to the sample.

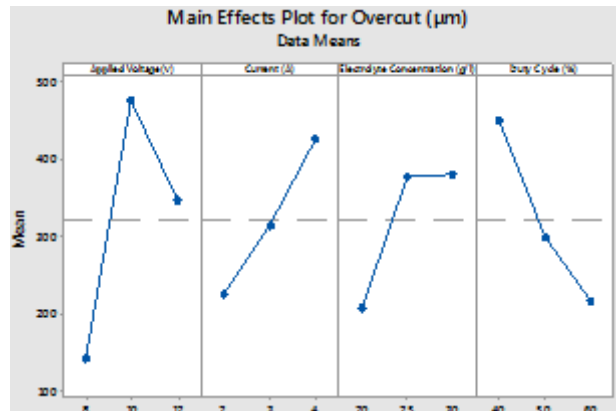


Fig. 8: Main effects for radial overcut



Fig. 9: Microscopic image for less accuracy

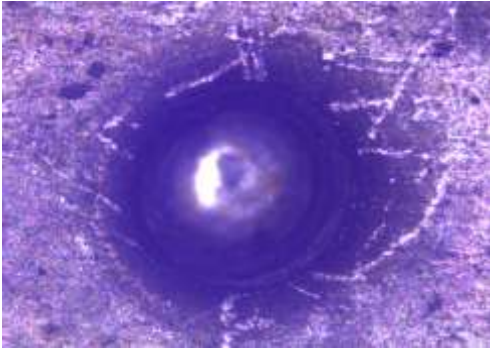


Fig. 10: Microscopic image for better

3.6. SEM analysis

The scanning electron microscope (SEM) uses a focused beam of high-energy electrons to generate a variety of signals at the surface of solid specimens. The signals that derive from electron-sample interactions reveal information about the sample including external texture, chemical composition, and crystalline structure and orientation of materials making up the sample. Fig. 11 shows the microscopic image of the least accurate machining. It is visible that the hole machined is not entirely spherical in nature. The material surrounding the hole has been slightly affected by the electrochemical reactions. The hole is not evenly circular in nature, in its depth and the slope of the boundary is also varying from side to side. Fig. 12 provides the most finely machined hole. The boundary is clearly defined in the hole. The surface around and in the hole is not affected by any stray electrochemical reactions and the image is rather crisp and clear. The slopes of the hole are steep like required and the circularity is maintained optimally. The material is finely removed and at a slower pace as well giving the better finish.

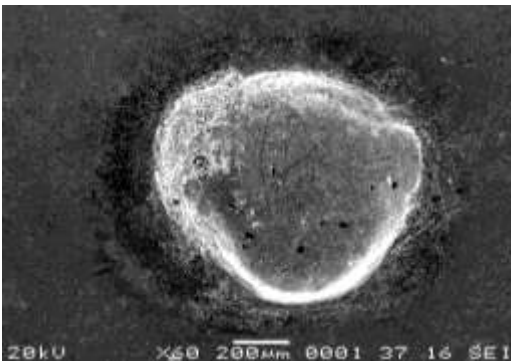


Fig. 11: SEM image for less accuracy

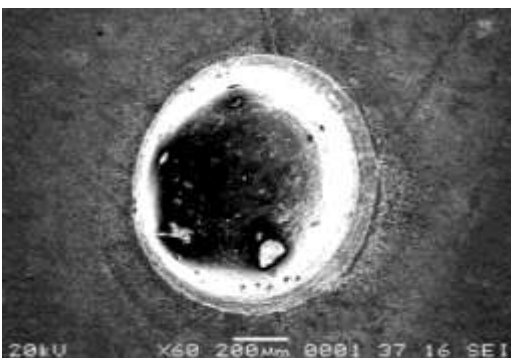


Fig. 12: SEM image for better

3.7. Confirmation test

After obtaining the optimized values for MRR, surface roughness and radial overcut, a confirmation test had been carried out to verify the integrity of the results obtained. The confirmatory test are carried out by setting up the applied voltage at 12V, current 4A, electrolyte concentration 25g/l, and duty cycle 40%. Finally, the satisfactory values of MRR is $1.878 \times 10^{-2} \text{ mm}^3/\text{min}$, surface roughness is $2.697 \mu\text{m}$, radial overcut is $612.724 \mu\text{m}$ and the confirmation test was carried out and then the error % of MRR is 4.525 %, error % of surface roughness is 2.636 % and error % of radial overcut is 3.455 %.

4. Conclusion

In this present work, Hastelloy C22 was machined using one of the on-traditional machining process called ECM. This alloy was chosen based on its prime application in heat exchangers. The input parameters - applied voltage, current, electrolyte concentration and duty cycle were suitably varied to get the optimum values of response parameters like metal removal rate, surface roughness, and radial overcut. The machining parameters were optimized using Grey-Taguchi approach and it was confirmed by conducting confirmation test. The graph which was generated using Minitab 17 software clearly represents the influence of each input parameter over the response parameter. We would like to conclude that the optimized satisfactory values are MRR is $1.878 \times 10^{-2} \text{ mm}^3/\text{min}$, surface roughness is $2.697 \mu\text{m}$, radial overcut is $612.724 \mu\text{m}$ under the condition of applied voltage at 12V, current 4A, electrolyte concentration 25g/lit, and duty cycle 40%. The following conclusions are drawn:

- The confirmation test was carried out and then the error % of MRR is 4.525%, error % of surface roughness is 2.636% and error % of radial overcut is 3.455%.
- As per micro tool was coated using epoxy coating the side current on the electrode was avoided thus giving rise to reduced overcut.
- The highest maximum-minimum grade value shows that the duty cycle has the most influence parameter on determining response characteristics.
- Through this experiment, we learned that Grey-Taguchi methodology can be effectively used to find the optimum levels of the machining parameters involved ECM process.

REFERENCES:

- [1] A. Singh, S. Anandita and S. Gangopadhyay. 2015. Microstructural analysis and multiresponse optimization during ECM of Inconel 825 using hybrid approach, *J. Materials and Mfg. Processes*, 30(7), 842-851.
- [2] B. Bhattacharyya, S. Mitra and A.K.B. Robotic. 2002. Electrochemical machining: new possibilities for micromachining, *Robotics and Computer Integrated Mfg.*, 18, 283-289. [https://doi.org/10.1016/S0736-5845\(02\)00019-4](https://doi.org/10.1016/S0736-5845(02)00019-4).
- [3] B. Bhattacharyya, J. Munda and M. Malapati. 2004. Advancement in electrochemical micro-machining, *Int. J.*

- Machine Tools & Manufacture*, 44, 1577-1589. <https://doi.org/10.1016/j.ijmachtools.2004.06.006>.
- [4] A.K.M. De Silva, H.S.J. Altena and J.A. McGeough. 2000. Precision ECM by process characteristic modelling, *CIRP Annals – Mfg. Tech.*, 49(1), 151-155.
- [5] A.K.M. De Silva, H.S.J. Altena and J.A. McGeough. 2003. Influence of electrolyte concentration on copying accuracy of precision - ECM, *CIRP Annals*, 52(1), 165-168. [https://doi.org/10.1016/S0007-8506\(07\)60556-3](https://doi.org/10.1016/S0007-8506(07)60556-3).
- [6] S. Dharmalingam, P. Marimuthu, K. Raja, R. Pandyrajan and R. Surendar. 2014. Optimization of process parameters on MRR and overcut in electrochemical micro machining on metal matrix composites using grey relational analysis, *Int. J. Engg. and Tech.*, 6(2), 519-529.
- [7] P. Govindan, M. Arjun, J. Arjun and S. Akshay. 2013. Analysis of electrochemical micromachining, *Int. J. Mgmt.*, 1, 5-14.
- [8] S. Gowri, P. Ranjithkumar, R. Vijayaraj and A.S.S. Balan. 2007. Micromachining: Technology for the future, *Int. J. Materials and Structural Integrity*, 1(1/2/3), 161-179.
- [9] J. Kozaka, K.P. Rajurkar and Y. Makkar. 2004. Selected problems of micro-electrochemical machining, *J. Materials Processing Tech.*, 149, 426-431. <https://doi.org/10.1016/j.jmatprotec.2004.02.031>.
- [10] F. Klockea, M. Zeisa, A. Klinka and D. Veselovaca. 2013. Experimental research on the electrochemical machining of modern titanium and nickel-based alloys for aero engine components, *The 17th CIRP Conf. Electro Physical and Chemical Machining, Proc. CIRP*, 6, 368-372.
- [11] T. Koyanoa and M. Kunieda. 2013. Ultra-short pulse ECM using electrostatic induction feeding method, *The 17th CIRP Conf. Electro Physical and Chemical Machining, Proc. CIRP*, 6, 390-394.
- [12] L. Guodong, L. Yong, K. Quancun and T. Hao. 2016. Selection and optimization of electrolyte for micro electrochemical machining on stainless steel 304, *18th CIRP Conf. Electro Physical and Chemical Machining, Proc. CIRP*, 42, 412-417.
- [13] L. Yong, Z. Yunfei, Y. Guang and P. Liangqiang. 2003. Localized electrochemical micromachining with gap control, *Sensors and Actuators*, 108, 144-148. [https://doi.org/10.1016/S0924-4247\(03\)00371-6](https://doi.org/10.1016/S0924-4247(03)00371-6).
- [14] M.M.K. Reddy. 2013. Influence of pulse period and duty ratio on electrochemical micro machining EMM characteristics, *Int. J. Mech. Engg. and Applications*, 1(4), 78-86. <https://doi.org/10.11648/j.ijmea.20130104.11>.
- [15] M.K. Dasa, K. Kumarb, T.Kr. Barmana and P. Sahooa. 2014. Optimization of surface roughness and MRR in electrochemical machining of EN31 tool steel using Grey-Taguchi approach, *Proc. Materials Sci.*, 6, 729-740. <https://doi.org/10.1016/j.mspro.2014.07.089>.
- [16] A.R. Mihalen and S.J. Harvey. 1986. Avoidance of macro surface defects in electrochemical machining (ECM) of steel work piece, *Advance Mfg. Tech.*, 374-380.
- [17] A. Mohanty, G. Talla, S. Dewangan and S. Gangopadhyay. 2014. Experimental study of material removal rate, surface roughness & microstructure in electrochemical machining of Inconel 825, *5th Int. & 26th All India Mfg. Tech., Design and Research Conf.*, 174(1-6).
- [18] N. Shibuya, Y. Ito and W. Natsu. 2012. Electrochemical machining of tungsten carbide alloy micro-pin with NaNO₃ solution, *Int. J. Precision Engg. and Mfg.*, 13(11), 2075-2078. <https://doi.org/10.1007/s12541-012-0273-2>.
- [19] W. Natsua and D. Kurahat. 2013. Influence of ECM pulse conditions on WC alloy micro-pin fabrication, *The 17th CIRP Conf. Electro Physical and Chemical Machining, Proc. CIRP*, 6, 401-406.
- [20] K.P. Rajurkar, M.M. Sundaram and A.P. Malshe. 2013. Review of electrochemical and electro discharge machining, *Proc. CIRP*, 6, 13-26. <https://doi.org/10.1016/j.procir.2013.03.002>.